Efficient spin-orbit torque switching of the semiconducting van der Waals ferromagnet $Cr_2Ge_2Te_6$

Vaibhav Ostwal[1,2], Tingting Shen[2,3], Joerg Appenzeller[1,2]
[1]Birck Nanotechnology Center, [2]Department of Electrical and Computer Engineering and [3]Department of Physics and Astronomy, Purdue University, West Lafayette, Indiana 47907, United States

Abstract:

Being able to electrically manipulate the magnetic properties in recently discovered van der Waals ferromagnets is essential for their integration in future spintronics devices. In this article, we study the magnetization of a semiconducting 2D ferromagnet, i.e. $Cr_2Ge_2Te_6$ using the anomalous Hall effect in $Cr_2Ge_2Te_6$/Tantalum heterostructures. Hysteresis and remanence in the magnetization loop with out-of-plane magnetic fields become more prominent the thinner the flakes. In order to manipulate the magnetization in such thin flakes a combination of an in-plane magnetic field and a charge current flowing through Ta – a heavy metal exhibiting giant spin Hall Effect – is used. In the presence of in-plane fields of 20 mT, charge current densities as low as 5×10^5 A/cm^2 are sufficient to switch the out-of-plane magnetization of $Cr_2Ge_2Te_6$. This finding highlights that current densities required for spin-orbit torque switching of $Cr_2Ge_2Te_6$ are about two orders of magnitude lower than those required for switching non-layered metallic ferromagnets such as CoFeB. The results presented here show the potential of 2D ferromagnets for low power memory and logic applications.

Introduction:

Newly discovered van der Waals (vdW) semiconducting materials such as CrI_3 [1] and $Cr_2Ge_2Te_6$ (CGT) [2] are shown to retain their ferromagnetic properties down to the monolayer limit. In case of semiconducting ferromagnets (FMs), previous studies have shown that electric fields (electrostatic doping) in such two-dimensional (2D) materials can manipulate the interlayer magnetic ordering in CrI_3[3][4] or impact the shape of the magnetization curves in case of CGT[5]. However, spin-torque manipulation of the magnetization in such semiconducting 2D-FMs has not been explored yet. Their high resistivity, atomically thin nature and the opportunity to achieve clean interfaces by stacking makes semiconducting FMs such as CGT an ideal candidate for spin-torque devices. Heavy metals (HMs) such as Pt or Ta with giant spin Hall angle (GSHE) are known to generate spin currents orthogonal to the flow of charge current through the HM. Such spin currents have been used to manipulate the magnetization of a number of ferromagnets in HM/FM heterostructures[6][7], generally referred to as spin-orbit torque (SOT) switching. In the context of SOT switching, where current shunting through the FM is undesirable, the semiconducting nature of 2D-FMs is expected to be especially useful. Examples of such envisioned spintronics devices include topological insulators (TIs) or transition metal dichalcogenides (TMDs) as channel materials with intrinsically high resistivity and strong spin-orbit-coupling (SOC) for generation of SOT. Note that while the electronic structure of TIs and TMDs is distinctly different due to the presence of topologically protected surface states in case of TIs, irrespective of the line-up of the Fermi level in these systems, their resistivities are always orders of magnitudes larger than those of metals. Moreover, the semiconducting nature of FMs may offer the opportunity of tuning the Fermi level with a gate and in this way impacting the magnetic properties simultaneously. In this article, we show for the first time SOT manipulation of semiconducting 2D-FM CGT.

Due to the semiconducting nature and low Curie temperature of CGT, direct electrical characterization of its magnetization has proven to be difficult, and most of the studies on CGT have utilized MOKE[2][5] or MFM[8]. A stack consisting of HMs such as Pt or W deposited on an insulating FM such as TMIG has shown to result in an induced anomalous Hall effect in the

metal, thus providing an electrical path towards reading the magnetization of insulating FMs[9][10]. In fact, a recent study has used a similar approach to characterize a CGT/Pt heterostructure[11]. In this article, we utilize the induced AHE in Ta to study the magnetization properties of CGT for various thicknesses. For thinner CGT films, we show by means of AHE that the out-of-plane magnetization (m_z) can be switched with a combination of SOT and in-plane magnetic fields similar to field-assisted magnetization switching in conventional metallic HM/FM films such as Ta/CoFeB/MgO. Our key finding is that SOT currents required for manipulation of the magnetization in a CGT/Ta system are almost two orders of magnitude smaller than in conventional metallic HM/FM systems.

Experimental Results and Discussion:

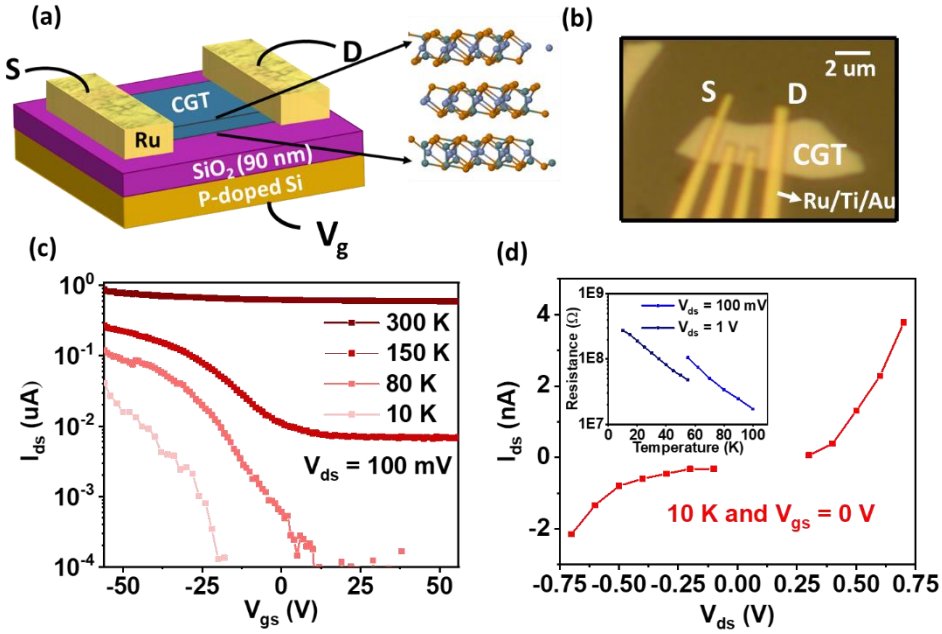

Figure 1. (a) 3D schematic of our back-gated FET with semiconducting CGT channel and Ru contacts. (b) Optical image of the actual device under investigation. (c) Transfer characteristics of the device for temperatures of 10 K, 80 K, 150 K and 300K for V_{ds}=100 mV. (d) non-linear I_{ds}-V_{ds} characteristics at 10 K for V_{gs}=0 V. (Inset: Temperature dependence of 2-terminal resistance of the device at V_{gs}=0 V.

To study the electrical properties of CGT, back-gated field-effect transistor (FET) structures with a 90nm SiO_2 gate-oxide were fabricated using standard scotch-tape exfoliation techniques on commercially purchased crystals. Immediately before sputtering the electron beam lithography defined source and drain Ruthenium (Ru) contacts, the CGT surface in the contact regions was mildly etched using an Ar plasma to remove the top CGT natural oxide layer to improve the contact quality. A schematic representation of the device layout and an optical image of the device structure are shown in fig1(a) and (b). Large work function Ru contacts are chosen, since transport in CGT is dominated by hole conduction through the p-branch [12][5]. Fig 1(c), shows transfer characteristics of the device for V_{ds} =100 mV for temperatures ranging from 10K to 300 K. A low on/off drain current (I_{ds}) ratio is observed in transfer characteristics at room temperature. However, at lower temperatures this ratio improves significantly. At 10 K, an on/off current ratio of ~$5*10^3$ is obtained for V_{ds}= 0.7 (shown in the supplementary info fig S1(a)). Note that such poor transfer characteristics at room temperature are consistent with previous reports of similar CGT FETs[5][11]. We suspect that the poor gate control at high temperatures is a result of oxidation of the top surface, which may result in the formation of a shunting channel. Fig 1(d) displays non-linear I_{ds}-V_{ds} characteristics that are expected in Schottky barrier dominated transistors. Moreover, the inset of fig1(d) shows the temperature dependent 2-terminal resistance of a CGT-FET at V_{gs} = 0 V for V_{ds} = 100 mV and 1V. The observed exponential dependence of resistance on temperature is consistent with the semiconducting nature of CGT. Note that 4-probe resistance measurements as a function of temperature show a similar exponential trend as the 2-terminal resistance in our FET structure

(shown in supplementary fig S1(b)), indicating that the temperature dependent behavior of the Schottky barriers is indeed not dominating the observed trends in case of the inset of fig1(d).

Next, we have performed temperature dependent Hall resistance measurements on the CGT/Ta heterostructure to study the magnetic properties of CGT. First, CGT flakes of various thicknesses are exfoliated onto a Si/SiO_2 substrate with 90 nm SiO_2. To avoid oxidation of the CGT flakes during the fabrication process, air exposure was limited to a few minutes after exfoliation and before the sample was mounted into the vacuum chamber for Ta deposition using a method similar to the one reported in [11]. In addition, a mild Ar plasma clean was performed to remove any oxide layer before depositing 5 nm of Ta using a magnetron sputtering tool (details are described in the experimental section). The actual Ta-Hall bar structures on the CGT were fabricated using e-beam lithography on a negative resist and Ar ion milling. Since the CGT thickness varies from flake to flake, etching was stopped just after etching the Ta layer, rather than etching the entire CGT areas, which are located outside the Ta-Hall bar masks. Since

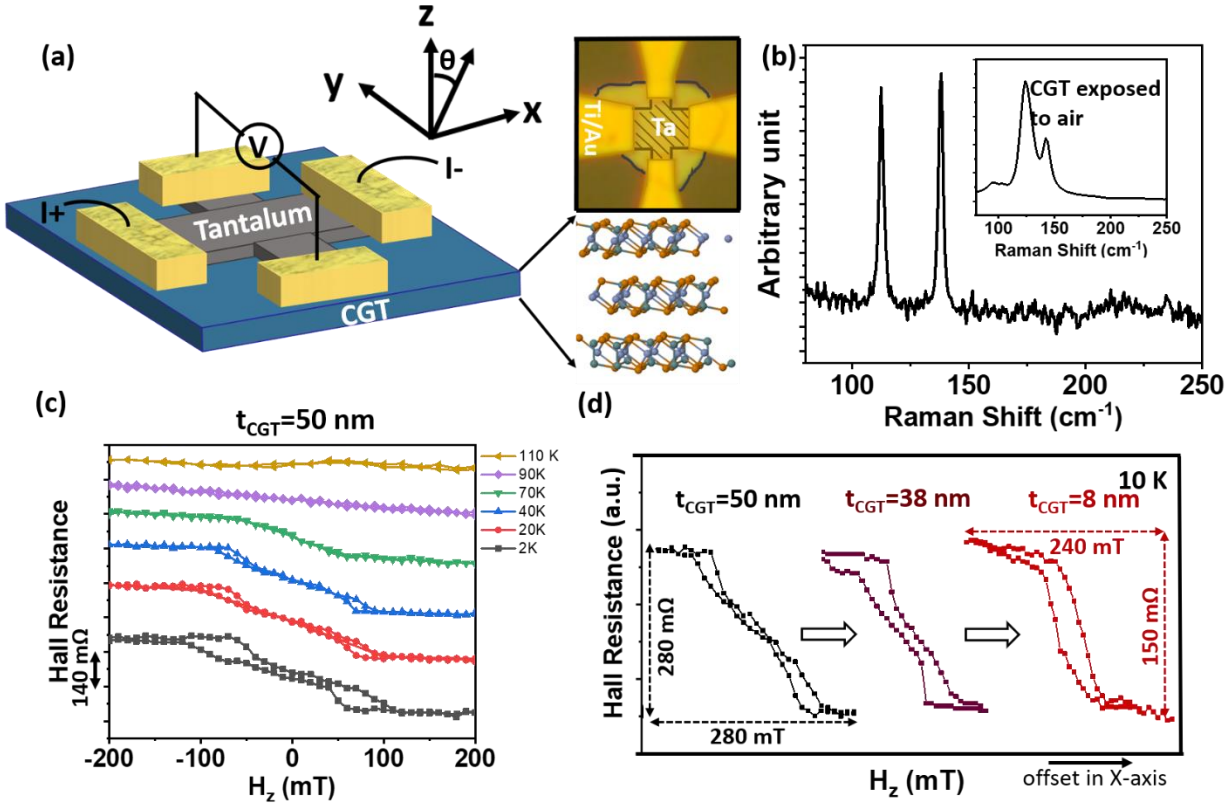

Figure 2. (a) 3D schematic and optical image of a fabricated Hall bar device from a CGT/Ta heterostructure and measurement set-up. (b) Raman spectrum of the CGT/Ta heterostructure device. (Inset: Raman spectrum of a CGT flake that was exposed to air.) (c) temperature dependent anomalous Hall resistance of the Hall bar device consisting of a 50 nm thick CGT layer under an applied out-of-plane magnetic field. The signature of an anomalous Hall effect starts to emerge at around 70 K, i.e. near the Curie temperature of CGT. (d) Normalized R_{AHE} for three different CGT thicknesses (t_{CGT}) (Dimensions of the Ta Hall bars used are indicated in the experimental section.)

CGT is highly insulating at low temperatures for V_{gs} = 0V if compared to Ta, current will pass exclusively through the patterned Ta-Hall bar. Finally, Ti/Au contacts were defined using a standard e-beam lithography and lift-off process. Fig 2(a) shows the measurement set-up and a representative optical image of a device. Temperature dependent Hall resistance measurements under out-of-plane (oop) magnetic fields (H_z) were performed using an excitation AC current (I_{ac}) of 10 uA and a lock-in set-up. Raman spectroscopy data were gathered to confirm the quality of the CGT films. Unlike the Raman spectra reported previously for CGT FETs, which

were exposed to air [12], the Raman spectra of our CGT/Ta Hall bar devices (with 50 nm CGT) show sharp peaks at approximately 112 cm^{-1} and 138 cm^{-1} (see fig 2(b)), consistent with previously reported Raman spectra on single crystal CGT [13][14]. Fig S2(a) (supplementary material) shows a similar Raman spectrum for a device from a thinner CGT flake, indicating that our process flow does ensure high quality devices even when thinner CGT flakes are employed. The surface roughness of the fabricated devices is in the sub-nanometer range even after the Ta deposition, further highlighting the process control achieved (see figure S2(b) in the supplementary materials section). Fig 2(c) shows the Hall resistance versus H_z for a Hall bar device from a 50 nm thick CGT flake. As apparent from fig 2(c), the anomalous Hall resistance (R_{AHE}), i.e. the out-of-plane magnetization (m_z) starts to emerge at around 70 K, near the expected Curie temperature of CGT[5][15]. Lower temperatures result in a larger hysteresis. However, even at 2K the magnetization remanence remains almost zero. Similar measurements were performed on devices from thinner CGT films (t_{CGT}). Normalized R_{AHE} curves at 10 K for t_{CGT} = 50 nm, 38 nm and 8 nm are displayed in figure 2(d). If compared with the CGT (50 nm)/Ta heterostructure (device #1), the R_{AHE} of a CGT (38 nm)/Ta heterostructure (device #2) and a CGT (8 nm)/Ta heterostructure (device #3) show progressively larger remanences with a much squarer shaped hysteresis as expected for a magnet with perpendicular magnetic anisotropy (PMA). Such thickness dependent magnetization curves have been observed previously using MOKE [5] and are here obtained using electrical measurements similar to [11].

Having demonstrated the PMA behavior of thin CGT flakes at low temperatures, we are in a position to explore the feasibility of SOT switching by means of currents through the Ta-layer in contact with the semiconducting magnet. When current is passed through a heavy metal that exhibits GSHE such as Ta using a configuration as displayed in fig3(a), spins generated at the interface are oriented in the y-direction and hence on their own cannot deterministically switch m_z due to symmetry reasons. However, an in-plane magnetic field applied along the current direction (H_x) can break the symmetry of the system and spin orbit torque can be utilized to deterministically switch m_z in this case. Hence, when the magnetic field is swept in the current direction (H_x) in the presence of a negative or positive DC current a clockwise or counterclockwise hysteresis loop of m_z results respectively [16][17] analogous to a charge current sweep under positive or negative magnetic fields H_x [7]. On the other hand, the same charge currents are not expected to result in any hysteresis loop if a magnetic field H_y is applied perpendicular to the current direction for our PMA magnet with its magnetization in the z-direction. Last, a current polarity independent hysteresis loop is expected if a magnetic field H_z is swept, a field that is in the same direction as the magnetization of the PMA magnet.

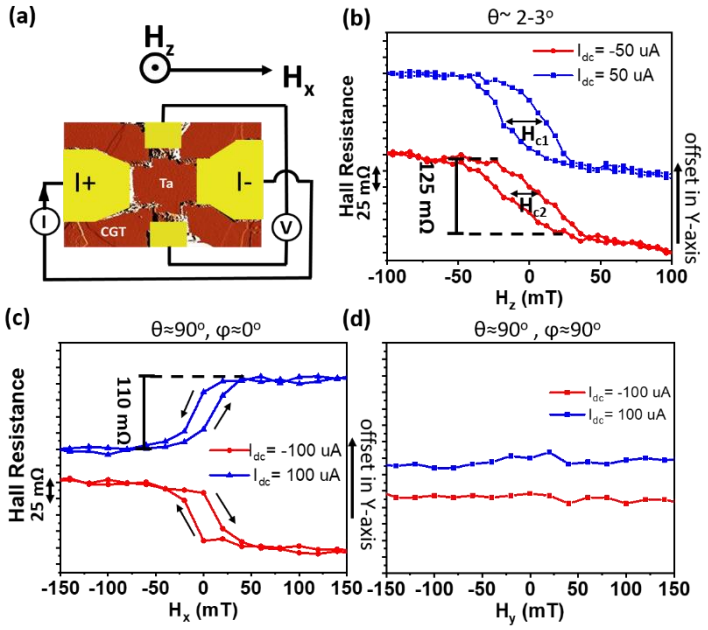

Figure 3. (a) AFM image of device #3 (b) Hall resistance versus H_z measured at I_{ac}= 4 uA using a lock-in set-up for I_{dc}=+/-50 uA. (c) Hall resistance versus H_x measured at I_{ac} = 4 uA using a lock-in set-up for I_{dc}=+/-100 uA. (d) Hall resistance versus H_x measured ath I_{ac}= 4 uA using a lock-in set-up for I_{dc}= +/-100 uA. All measurements were performed at 10K.

Exactly these three sets of experiments are displayed in figures 3(b), (c) and (d). The Hall resistance of device #3 (AFM image is shown in fig 3(a)) was measured at 10K with an I_{ac}=4 uA, using a lock-in set-up in the presence of DC currents (I_{dc}) of different magnitude and polarization. Magnetic fields are swept in the x-, y-, and z-direction respectively as discussed above. The observed behavior is largely consistent with the expressed expectations under different magnetic field and charge current conditions. As shown in fig 3(c), while sweeping H_x, R_{AHE} (i.e. m_z) switching loops are observed even in the absence of H_z and the polarity of the switching loops is reversed between I_{dc}=+100 uA and –100 uA. Note that the counterclockwise and clockwise switching under positive and negative charge currents, respectively, is opposite compared to Ta/CoFeB [7] and W/CoFeB [18] systems due to an inversion of the stacking sequence of HM and FM layers. Our observations are also consistent with the observed SOT switching in a $Tm_3Fe_5O_{12}$/Tungsten (TMIG/W) heterostructure as reported before [9], since W in their experiments and Ta in our experiments exhibit a spin Hall angle with the same polarity. On the other hand, no such R_{AHE} loops are observed while sweeping H_y (fig 3(d)).

Moreover, while we do not observe a change in the polarity of hysteresis loop when scanning H_z under different current polarities, we did notice a change of the coercive field under these two different DC currents. This effect has been discussed before in references [16] and [17] that attribute their observation to a slight misalignment of the external magnetic field relative to the intended z-orientation. A small misalignment of θ~2-3° that results in a small magnetic field component in the x-direction (which is unintentional in our custom-built probe for the PPMS system) is sufficient to explain the change in coercivity. Such a change in coercivity is a manifestation of damping-like torque which is expected from the GSHE in 5 nm thick Ta films. In the supplementary information under S3, we have estimated the spin-orbit field of the heterostructure using this coercivity change for +50 and -50 uA, based on the method described in ref [16][17]. In general, to study effective SOT fields in metallic bilayers of HM/FM stacks under excitation of AC currents (I_w), the second harmonic of the Hall voltage (V_{2w}) is measured. However, for our HM/insulating-FM system comparatively large thermoelectric effects such as the spin Seebeck effect dominate V_{2w}. This is the reason why we observe in our heterostructure a sigmoidal shape of V_{2w} with respect to an in-plane magnetic field (H_x) (supplementary figS4), similar to what has been previously reported for a TMIG/Pt system [19]. Such a sigmoidal dependence is expected due to larger spin Seebeck effect compared to the signal generated from effective SOT fields in our heterostructure. Note that the

presence of contributions from thermoelectric effects does not imply the absence of contributions from effective spin-torque fields. However, distinguishing these two components is challenging due to the magnitude of the thermoelectric effects in our sample. Hence, we have focused our experiments on the direct observation of SOT switching rather than analyzing effective SOT fields. The sum of these experimental findings unambiguously proves the successful SOT switching in a Ta/CGT heterostructure that is reported here for the first time.

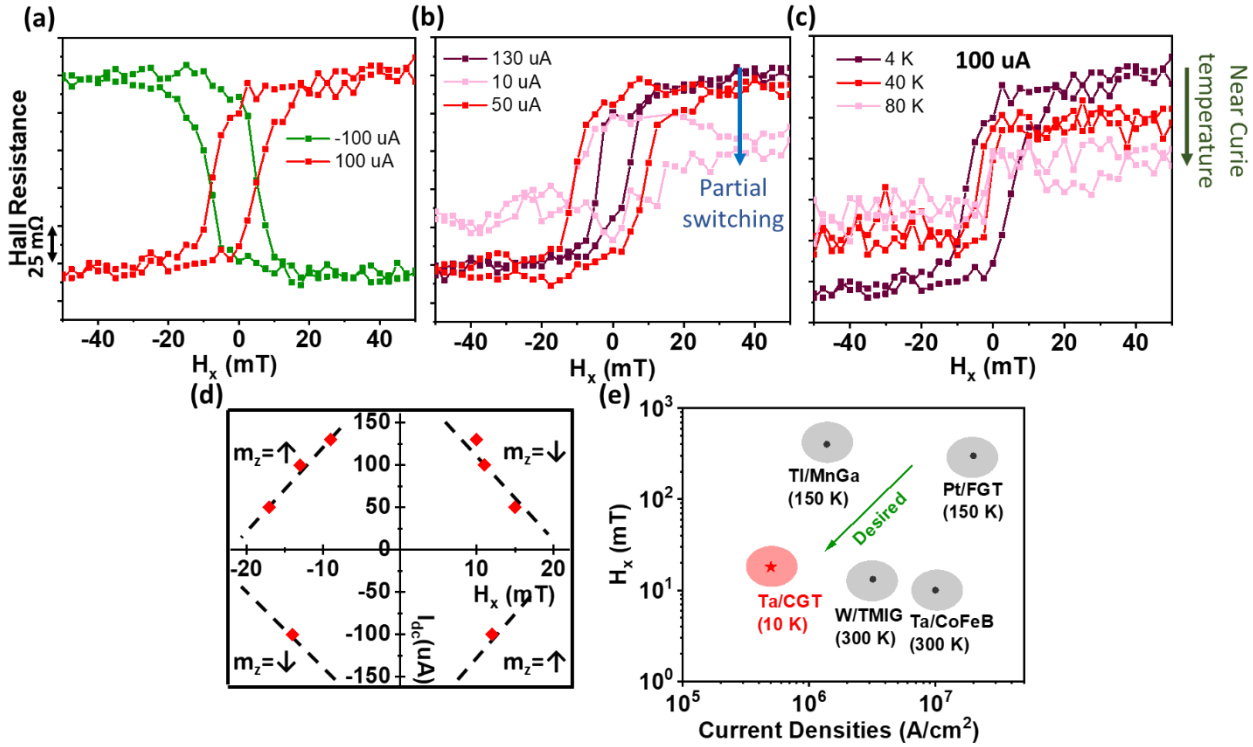

Figure 4. (a) Field assisted SOT switching of out-of-plane magnetization with I_{dc}= +/- 100 uA at 4K. (b) I_{dc} dependent field assisted SOT switching at 4K. (c) Temperature dependent field assisted SOT switching at T=4 K, 40 K and 80 K. (d) Phase diagram of m_z for applied combinations of I_{dc} and H_x at 4 K (e) Current densities and in-plane fields required for SOT switching of previously reported magnetic heterostructures in comparison to this work. Values in brackets denote the temperatures at which experiments were performed.

Next, we are interested in exploring how efficient the charge-to-spin conversion in our Ta/CGT stacks is in comparison to the reported SOT switching in other heterostructures. Figure 4 shows device characteristics of yet another Ta/CGT device (device #4 with estimated thickness of 8-12 nm – also see figure S5 in the supplementary material section). As in the case discussed in the context of figure 3(c), clear SOT switching with the expected reversal of the hysteresis loop is observed in figure 4(a) when sweeping H_x under positive and negative charge current polarities at 4K. Moreover, as expected from previous studies [10], higher charge currents require smaller H_x and vice versa to change the magnetization of our CGT magnet with PMA (see figure 4(b)). Note that too small I_{dc}-values result in incomplete (partial) reversal of the magnetization direction since in a large FM with a size of a few μm^2, such as in our experiment, SOT switching is driven by domain nucleation [20,21][22]. Furthermore, the low coercivity and low remanence in the magnetization loops of CGT films (fig 2(d)) suggest that domain nucleation is easier for CGT films if compared to ferromagnets such as CoFeB or TMIG which show sharp switching at coercivity. We believe that this could be one of the possible reasons for the low current densities required for SOT switching in our experiments. However, out-of-plane fields required for magnetization saturation are not small (around 50 mT as shown in

figure 3(b)) which suggest even though nucleation is easier, SOT switching of total magnetization would require substantial effective fields and further investigation is required to understand SOT switching mechanism in these micron-scale devices. Plotting the actual I_{dc} and critical H_x-fields for complete switching allows creating a switching phase diagram – figure 4(d) that shows the typical diamond shape [18]. Current and magnetic field value pairs outside the diamond guarantee SOT switching. In the presence of an in-plane field of approximately 20 mT an I_{dc}-value of 50 uA, which corresponds to a current density of around $5*10^5$ A/cm^2 is sufficient to switch m_z. To further evaluate the SOT switching, we have also characterized device#4 for temperatures of 40K and 80 K. Since the magnetization switching of our micro-scale device is a thermally assisted process (along with a lowered magnetic anisotropy at higher temperatures), we expect easier magnetization switching, i.e. lower in-plane fields required for switching at higher temperatures. This behavior is observed in fig 4(c) for a constant current of 100 uA. At 80 K, a negligible R_{AHE} loop is observed due to the loss of ferromagnetism near the Curie temperature of CGT. Figure 4(e) puts our experimental findings on SOT switching into the context of previously reported data on other hetero stacks. It is apparent that metallic heavy metal/ ferromagnet (HM/FM) heterostructures such as Ta/CoFeB [7] or Pt/FGT [23][24] require in general high critical current densities of around 10^7 A/cm^2 for field-assisted SOT switching as a result of current shunting through the magnet and large M_s-values of the magnets used. On the other hand, integration of insulating FMs such as TMIG [9] or usage of TI as GSHE material that exhibits large spin Hall angles [16] can reduce the required critical current densities to ~10^6 A/cm^2. Here, using semiconducting 2D-FM CGT, we have shown that even lower critical current densities of ~$5*10^5$ A/cm^2 can be sufficient for field-assisted SOT switching.

We believe that the reason for the further reduced current densities in our structures lies in the quality of the films and interfaces. TMIG films (which are usually grown on $Nd_3Ga_5O_{12}$) suffer from finite size and strong surface modification effects, which collectively reduce the saturation magnetization (M_s) in such films [9]. In contrast, in the case of CGT, which is a van der Waals (vdW) material, the two-dimensional bond structure results in a much lower defect density and better crystallinity even for ultra-thin flakes. This in turn allows for cleaner interfaces and an almost unchanged M_s-value even in mono-layers[15] ultimately improving the SOT efficiency. Moreover, parameters such as magnetic damping constant and spin mixing intermixing conductance directly affect the critical SOT current densities required, which are as of yet unknown for thin CGT films. Our experimental findings that low switching current densities are sufficient to impact the magnetization of CGT underscores the importance to theoretically explore the spin torque switching mechanism of 2D vdW magnets as literature on this topic is scarce.

Conclusion:

In conclusion, by integrating semiconducting vdW ferromagnets and heavy metals with high SOC, we have demonstrated strong spin-orbit torque effects in CGT/Ta heterostructures. In particular, in the presence of an in-plane magnetic field, the out-of-plane magnetization of CGT can be manipulated by flowing a charge current through Tantalum. Current densities as low as $5*10^5$ A/cm^2 are sufficient for SOT switching in the presence of in-plane fields of 20 mT. Spin-torque switching as demonstrated here along with the previously explored gate voltage manipulation of 2D semiconducting FMs may enable novel vdW heterostructures for the realization of novel low power spintronic devices for memory and logic applications.

References:

[1] B. Huang, G. Clark, E. Navarro-Moratalla, D. R. Klein, R. Cheng, K. L. Seyler, D. Zhong, E. Schmidgall, M. A. McGuire, D. H. Cobden, W. Yao, Di. Xiao, P. Jarillo-Herrero, X. Xu, *Nature* **2017**, *546*, 270.

[2] C. Gong, L. Li, Z. Li, H. Ji, A. Stern, Y. Xia, T. Cao, W. Bao, C. Wang, Y. Wang, Z. Q. Qiu, R.

J. Cava, S. G. Louie, J. Xia, X. Zhang, *Nature* **2017**, *546*, 265.
[3] B. Huang, G. Clark, D. R. Klein, D. MacNeill, E. Navarro-Moratalla, K. L. Seyler, N. Wilson, M. A. McGuire, D. H. Cobden, D. Xiao, W. Yao, P. Jarillo-Herrero, X. Xu, *Nat. Nanotechnol.* **2018**, *13*, 544.
[4] S. Jiang, L. Li, Z. Wang, K. F. Mak, J. Shan, *Nat. Nanotechnol.* **2018**, *13*, 549.
[5] Z. Wang, T. Zhang, M. Ding, B. Dong, Y. Li, M. Chen, X. Li, J. Huang, H. Wang, X. Zhao, Y. Li, D. Li, C. Jia, L. Sun, H. Guo, Y. Ye, D. Sun, Y. Chen, T. Yang, J. Zhang, S. Ono, Z. Han, Z. Zhang, *Nat. Nanotechnol.* **2018**, *13*, 554.
[6] I. M. Miron, K. Garello, G. Gaudin, P.-J. Zermatten, M. V Costache, S. Auffret, S. Bandiera, B. Rodmacq, A. Schuhl, P. Gambardella, *Nature* **2011**, *476*, 189.
[7] L. Liu, C. Pai, Y. Li, H. W. Tseng, D. C. Ralph, R. A. Buhrman, S. Science, N. Series, N. May, *Science (80-.).* **2012**, *336*, 555.
[8] T. Guo, Z. Ma, G. Lin, X. Luo, Y. Hou, Y. Sun, Z. Sheng, Q. Lu, *arXiv* **2018**, 1803.06113.
[9] Q. Shao, C. Tang, G. Yu, A. Navabi, H. Wu, C. He, J. Li, P. Upadhyaya, P. Zhang, S. A. Razavi, Q. L. He, Y. Liu, P. Yang, S. K. Kim, C. Zheng, Y. Liu, L. Pan, R. K. Lake, X. Han, Y. Tserkovnyak, J. Shi, K. L. Wang, *Nat. Commun.* **2018**, *9*, 3612.
[10] C. O. Avci, A. Quindeau, C. F. Pai, M. Mann, L. Caretta, A. S. Tang, M. C. Onbasli, C. A. Ross, G. S. D. Beach, *Nat. Mater.* **2017**, *16*, 309.
[11] M. Lohmann, T. Su, B. Niu, Y. Hou, M. Alghamdi, M. Aldosary, W. Xing, J. Zhong, S. Jia, W. Han, R. Wu, Y. T. Cui, J. Shi, *Nano Lett.* **2019**, *19*, 2397.
[12] W. Xing, Y. Chen, P. M. Odenthal, X. Zhang, W. Yuan, T. Su, Q. Song, T. Wang, J. Zhong, S. Jia, X. C. Xie, Y. Li, W. Han, *2D Mater.* **2017**, *4*, 024009.
[13] A. Milosavljević, A. Šolajić, J. Pešić, Y. Liu, C. Petrovic, N. Lazarević, Z. V. Popović, *Phys. Rev. B* **2018**, *98*, 104306.
[14] Y. Tian, H. Ji, R. J. C. L. D. Alegria, J. R. Petta, K. S. Burch, *arXiv* **2014**, 1410.1898.
[15] M. Mogi, A. Tsukazaki, Y. Kaneko, R. Yoshimi, K. S. Takahashi, M. Kawasaki, Y. Tokura, *APL Mater.* **2018**, *6*, 091104.
[16] H. D. K. Nguyen, U. Yugo, N. H. Pham, *Nat. Mater.* **2018**, *17*, 808.
[17] P. Li, T. Liu, H. Chang, A. Kalitsov, W. Zhang, G. Csaba, W. Li, D. Richardson, A. DeMann, G. Rimal, H. Dey, J. S. Jiang, W. Porod, S. B. Field, J. Tang, M. C. Marconi, A. Hoffmann, O. Mryasov, M. Wu, *Nat. Commun.* **2016**, *7*, 12688.
[18] Q. Hao, G. Xiao, *Phys. Rev. Appl.* **2015**, *3*, 034009.
[19] C. O. Avci, A. Quindeau, C. F. Pai, M. Mann, L. Caretta, A. S. Tang, M. C. Onbasli, C. A. Ross, G. S. D. Beach, *Nat. Mater.* **2017**, *16*, 309.
[20] J. Cao, Y. Chen, T. Jin, W. Gan, Y. Wang, Y. Zheng, H. Lv, S. Cardoso, D. Wei, W. S. Lew, *Sci. Rep.* **2018**, *8*, 1355.
[21] S. Woo, M. Mann, A. J. Tan, L. Caretta, G. S. D. Beach, *Appl. Phys. Lett.* **2014**, *105*, 212404.
[22] O. J. Lee, L. Q. Liu, C. F. Pai, Y. Li, H. W. Tseng, P. G. Gowtham, J. P. Park, D. C. Ralph, R. A. Buhrman, *Phys. Rev. B - Condens. Matter Mater. Phys.* **2014**, *89*, 024418.
[23] X. Wang, J. Tang, X. Xia, C. He, J. Zhang, Y. Liu, C. Wan, C. Fang, C. Guo, W. Yang, Y. Guang, X. Zhang, H. Xu, J. Wei, M. Liao, X. Lu, J. Feng, X. Li, Y. Peng, H. Wei, R. Yang, D. Shi, X. Zhang, Z. Han, Z. Zhang, G. Zhang, G. Yu, X. Han, *arXiv* **2019**, 1902.05794.
[24] M. Alghamdi, M. Lohmann, J. Li, P. R. Jothi, Q. Shao, M. A. 1#, T. Su, B. Fokwa, J. Shi, *arXiv* **2019**, 1903.00571.

Acknowledgements:

The authors would like to thank Prof. Pramey Upadhyaya and Mushfiqur Rahman for many fruitful discussions and their feedback on this work. This work was supported in part by the Center for Probabilistic Spin Logic for Low-Energy Boolean and Non-Boolean Computing (CAPSL), one of the Nanoelectronic Computing Research (nCORE) Centers as task 2759.003 and 2759.004, a Semiconductor Research Corporation (SRC) program sponsored by the NSF through CCF 1739635.

Methods:

Device fabrication details: Contacts to the CGT-FET structure were defined by e-beam lithography using a bilayer of PMMA (495/950) as a positive resist. Ruthenium contacts (~15nm) were deposited in a PVD sputtering tool at a chamber base-pressure of ~$3*10^{-8}$ Torr. Before sputtering Ru as contacts for the FET structures, the CGT surface was etched with an Ar plasma (15 W) for 45 sec to remove any top oxide layer. Finally, Ti(10nm)/Au(80nm) was evaporated onto the Ru contact required for wire bonding purposes. To prepare the CGT/Ta heterostructures, Si/SiO_2 substrates with exfoliated CGT flakes were transferred to the sputter tool immediately after exfoliation. Samples were heated to 100^{o}C to remove any water vapor that may have accumulated on the surface. Next, the samples were exposed to a mild Ar plasma (same conditions as described above) to remove any top oxide layer as mentioned before and then Tantalum (5 nm) was sputtered. The dimensions of the Ta Hall bars for devices 1 and 2 are approximately 4.5 um (width) * 9 um (length), while they are approximately 2 um * 4 um for devices 3 and 4.

Measurement details:

All electrical measurements were performed with a PPMS tool from Quantum Design. FET transfer and output curves were measured using two voltage sources (V_{GS} and V_{DS}) Keithely-2400s. To measure the Hall resistance of the CGT/Ta heterostructure, a Keithley 6221 was used as an AC current source at a frequency of 97.7 Hz while a SR830 digital lock-in set-up is used to measure the Hall voltage. In the SOT switching experiments, a Keithley 6221 was used as an AC+DC current source. To change the angle θ as defined in figure 2(a) between the external magnetic field and the current direction through the device, sample holder was manually rotated before loading the sample into the PPMS chamber again.